Zirconium Doped Titania: Destruction of Warfare Agents and Photocatalytic Degradation of Orange 2 Dye

V. Štengl[1,*], S. Bakardjieva[1], N. Murafa[1] and F. Opluštil[2]

[1]*Institute of Inorganic Chemistry AS CR v.v.i., 250 68 Řež, Czech Republic and* [2]*Military Technical Institute of Protection Brno, Veslařská 230, 628 00 Brno, Czech Republic*

Abstract: The homogeneous hydrolysis mixture of titanium oxo-sulphate and zirconium oxo-sulphate with urea at temperature 100°C has been used to prepare Zr^{4+} doped anatase with high specific surface area. The structure of the prepared samples was determined by X-ray powder diffraction (XRD) and selected area electron diffraction (SAED). The morphology and microstructure characteristics were also obtained by scanning electron microscopy (SEM) and high resolution electron microscopy (HRTEM). The nitrogen adsorption-desorption was used for surface area (BET) and porosity determination. These oxides were taken for experimental evaluation of their reactivity with yperite (2,2´-dichloroethyl sulfide or HD or sulphur mustard), soman (3,3-dimethyl-2-butyl methylphosphonofluoridate or GD) and matter VX (O-ethyl S-2-(diisopropylamino)ethyl methylphosphonothionate). The photoactivity of the prepared samples was assessed by the photocatalytic decomposition of Orange 2 dye in an aqueous slurry under irradiation of 254 nm and 365 nm wavelength.

Key Words: Anatase, mustard gas, soman, VX, detoxification agents, chemical warfare agents, photocatalysis.

1. INTRODUCTION

Nano-sized inorganic oxides are regarded as promising non-aggressive reagents usable for treatment of sensitive materials contaminated with lethally toxic chemical agents, namely the nerve agents, such as sarin (2-(fluoro-methylphosphoryl)-oxypropane or O-isopropyl methylphosphono-fluoridate or GB), soman (3,3-dimethyl-2-butyl methylphosphonofluoridate or 3-(fluoro-methyl-phosphoryl)oxy-2,2-dimethyl-butane or GD) and matter VX (O-ethyl S-2-(diisopropylamino)ethyl methyl-phosphonothionate or VX) as well as blistering agents (e.g. yperite (2,2´-dichloroethyl sulfide or HD or sulphur mustard). The detoxification capability of those highly dispersed oxides (e.g. MgO, CaO, ZnO, AlO_x $(OH)_y$, ZrO_2, TiO_2) has been extensively studied and reported [1-5]. The reactivity with warfare agents of the nanosized MgO nanoparticles prepared by an autoclave hypercritical drying procedure from $Mg(OCH_3)$ [6] and nanosized alumina (α-Al_2O_3) [7] from aluminium sec. butoxide has been studied. On the basis of the results mentioned in [8] a simple preparation method of spherical, uniform particles of Al^{3+}, Fe^{3+}, Cr^{3+} and Ti^{4+} was designed. The investigation of homogeneous precipitation process of metal sulphates with urea at temperature 95-100°C in aqueous solutions generating spherical particles was described in [9]. The authors used this method for preparation of spherical particles of anatase and ferrihydrite for destruction of warfare agents [10] or photocatalytic degradation of 4-chlorphenol [11]. The same method for preparation of nanodispersive mixed oxides of Ti, Zn, Al and Fe was used and destruction of warfare

agents was tested [12]. Zr^{4+} doped TiO_2 nanopowder with high photocatalytic activity can be successfully prepared by sol–gel method using titanium(IV) isopropoxide and zirconium nitrate as precursors [13]. In the paper [14], Zr^{4+}-doped TiO_2 nanocrystal was prepared by sol–gel method and Zr^{4+} was introduced in the form of inorganic salt $ZrOCl_2$. The results showed that low-amount presence of Zr^{4+} could suppress the growth of TiO_2 grains, raise the surface area, and accelerate surface hydroxylation, which resulted in the higher photocatalytic activity of the doped TiO_2. Highly stable ZrO_2–TiO_2 mixed oxides were prepared by co-precipitation method taking $ZrOCl_2$ and $TiCl_4$ as the precursor materials in the mixture of acetyl acetone, ethyl alcohol and ammonium hydroxide [15]. Anatase-type TiO_2 doped with 4.7 and 12.4 mol% ZrO_2 that were directly precipitated as nanometer-sized particles from acidity precursor solutions of $TiOSO_4$ and $Zr(SO_4)_2$ by simultaneous hydrolysis under hydrothermal conditions at 200°C [16]. Highly crystalline and surface-modified Zr-doped TiO_2 nanorods were successfully prepared using a non-hydrolytic sol–gel method that involves the condensation of metal halides with alkoxides in anhydrous trioctylphosphine oxide (TOPO) at either 320 or 400 °C [17]. The ordered porous mixed Ti and Zr oxides were prepared by direct synthesis through the surfactant templating route. The titanium sources were titanium isopropoxide, $Zr(SO_4)\cdot 4H_2O$ as the zirconium source and hexadecyltrimethyl-ammonium bromide (C_{16}TMABr) as the surfactant [18]. Titania–zirconia mixed oxides with various ZrO_2 content in TiO_2 (10, 50 and 90 wt.%) were prepared by the sol–gel method [19]. Spherical particles of zirconia were obtained by the calcination of monodisperse oxy-basic zirconium carbonate $Zr_2O_2(OH)_2\cdot CO_3\cdot 2H_2O$ particles produced by homogeneous precipitation from zirconium sulphate solutions [20].

*Address correspondence to this author at the Institute of Inorganic Chemistry ASCR v.v.i., Husinec-Rez, 250 68, Czech Republic; Tel: +042-2-6617-3144; Fax: +042-2-2094-1502; E-mail: stengl@iic.cas.cz

In the present study, Zr^{4+} doped TiO_2 having stable anatase-type structure, was directly synthesized from aqueous solutions of $TiOSO_4$ and $ZrOSO_4$ by homogeneous hydrolysis with urea as nanometer sized particles agglomerated in spherical clusters. The prepared nanodispersive oxides were used for experimental evaluation of their reactivity with sulphur mustard, soman and matter VX. The photoactivity of the prepared Zr^{4+} doped titania was assessed by the photocatalytic decomposition of Orange 2 dye in an aqueous slurry under irradiation of 254 nm and 365 nm wavelength.

2. EXPERIMENTAL

2.1. Preparation of Zr Doped Titania Samples

All chemical reagents used in the present experiments were obtained from commercial sources and used without further purification. $TiOSO_4$, $ZrCl_4$ and urea were supplied by Fluka, Munich, Germany.

$ZrOSO_4$ was prepared by a reaction stoicheiometric amount of $ZrCl_4$ and sulphuric acid. $ZrCl_4$ was dissolved in 98% sulphuric acid in a crystal dish and heated at temperature 100°C until HCl escaped from the reaction mixture. Next reaction mixture was boiled down to crystallization. The pure $ZrOSO_4$ (ICDD PDF 01-0366) for the next reaction was used. The Zr^{4+} doped nanocrystalline titania was prepared by homogeneous hydrolysis of $TiOSO_4$ and $ZrOSO_4$ aqueous solutions using urea as the precipitation agent. In a typical process, 100g $TiOSO_4$ was dissolved in 100 mL hot distilled water acidified with 98% H_2SO_4. The pellucid liquid was diluted into 4 L of distilled water, added defined amount of $ZrOSO_4$ (see Table **1**) and mixed with 400 g of urea. The mixture was heated to 100 °C under stirring and kept at this temperature for 9 h until pH 7 was reached and ammonia escaped from the solution. The formed precipitates have been washed by distilled water with decantation, filtered off and dried at temperature 105 °C in a dry oven. By this method there were prepared six samples denoted as TiZr_1 - TiZr_6.

2.2. Characteristic Methods

Surface area of the samples outgassed for 15 min at 120 °C was determined from nitrogen adsorption-desorption isotherms at liquid nitrogen temperature using a Quantachrom Nova 42000e instrument. Langmuir B.E.T. method was used for surface area calculation [21], while pore size distribution (pore diameter and volume) was determined by the B.J.H. method [22].

Transmission electron microscopy (TEM and HRTEM) micrographs were obtained by using two instruments, namely Philips EM 201 at 80 kV and JEOL JEM 3010 at 300 kV (LaB_6 cathode). Copper grid coated with a holey carbon support film was used to prepare samples for the TEM observation. A powdered sample was dispersed in ethanol and the suspension was treated in an ultrasonic bath for 3 minutes.

Scanning electron microscopy (SEM) studies were performed using a Philips XL30 CP microscope equipped with EDX (energy dispersive X-ray), Robinson, SE (secondary electron) and BSE (back-scattered electron) detectors. The sample was placed on an adhesive C slice and coated with Au-Pd alloy 10 nm thick layer.

X-ray diffraction (XRD) patterns were obtained by Siemens D5005 instrument using Cu Kα radiation (40 kV, 30 mA) and diffracted beam monochromator. Qualitative analysis was performed with the Eva Application and the Xpert HighScore using the JCPDS PDF-2 database [23]. The crystallite size of the samples was calculated from the Scherrer equation [24] using the X-ray diffraction peak at $2\Theta = 25.4°$ (anatase).

Infrared spectra were recorded by using Thermo-Nicolet Nexus 670 FT-IR spectrometer approximately in 4000-500 and 500-50 cm^{-1}, respectively, with single-reflection horizontal accessory on Si crystal. The samples were prepared in a form of pellets in KBr at ambient conditions and measured in the transmission mode.

Photocatalytic activity of samples was assessed from the kinetics of the photocatalytic degradation of 0.02 M Orange 2 dye (also known as Acid Orange 7, sodium salt 4-[(2-hydroxy-1-naphtenyl)azo]-benzenesulfonic acid) in aqueous slurries. Kinetics of the photocatalytic degradation of aqueous Orange 2 dye solution was measured by using a self-constructed photoreactor [25, 26]. The photoreactor consists of a stainless steel cover and quartz tube with a florescent lamp (254 nm and 365 nm). Its power is 13W. Orange 2 dye solution circulated by means of membrane pump through flow cuvette. The concentration of Orange 2 dye was determined by measuring absorbance at 480 nm with VIS spectrofotometer ColorQuestXE.

2.3. Method of Warfare Agents Disintegrations

The samples of zirconium oxide doped titania were evaluated for their ability to convert sulphur mustard (if you like soman and matter VX) into non-toxic products. Synthesised powdery samples were dried over 24 hour in a vacuum kiln (at 100 °C, 400 Pa) before tests. Weighed portion of the given evaluated nanosized sample was put into a glass vial provided with a screw solid cap (Supelco, type CRS-33). The toxic agent was dosed onto the powder reagent layer in the form of a solution in a chosen solvent. The vial was sealed with a cap and put into a thermostat. All experiments were performed at 25 °C, and each run was repeated four to six times. Adding of isopropylalcohol (2 mL) terminated the reaction. Suspension was vigorously agitated and liquid fraction was separated from the solid using a centrifuge (6 000 cc. min^{-1} for 3 minutes), and subsequently analysed for a residual content of the mustard. The respective detoxification capabilities of the evaluated samples were expressed as percentages of mustard elimination from the reaction mixture under the given experimental conditions. The concentration of sulphur mustard was quantified by method of Franke [27] and concentration of nervous agents (soman, VX) by biochemical method with colourmetric determination of thiols according to Ellman [28].

3. RESULTS AND DISCUSSION

3.1. X-Ray Diffraction (XRD)

The powder XRD patterns of the Zr^{4+} doped titania prepared by homogeneous hydrolysis of oxo-sulphates with urea are shown in Fig. (**1**). From the XRD patterns and the corresponding characteristic 2Θ values of the diffraction peaks, it can be confirmed that TiO_2 in as prepared samples

is identified as an anatase-phase (ICDD PDF 21-1272). No other polymorphs of titania are observed. The broadening of diffraction peaks indicates a small size of nanocrystals titania. The average size t of crystallites was calculated from the peak half-width B, using the Sherrer equation [24],

$$t = \frac{k\lambda}{B\cos\theta} \qquad (1)$$

where k is a shape factor of the particle (it is *1* if the spherical shape is assumed), λ and Θ are the wavelength and the incident angle of the X-rays, respectively. The peak width was measured at half of the maximum intensity. The crystallite size was calculated from a diffraction plane (101) of anatase and increased with the amount of Zr. The crystallite size obtained by XRD corresponds with particle size from HRTEM micrographs (see Fig. **4** and Table **1**). The unit cell parameters a and c increased with the content of Zr and this fact indicated incorporation of Zr to lattice of anatase. The diffraction patterns obtained for samples denoted TiZr6 and TiZr7 respectively, are characteristic for amorphous phase. The collapse of samples crystallinity depended on the amount of Zr. During the hydrolysis the complexes such as $[Zr(OH)_n]^{4-n}$ could prevent the formation of crystalline particles and thus lead to gel precipitation [29].
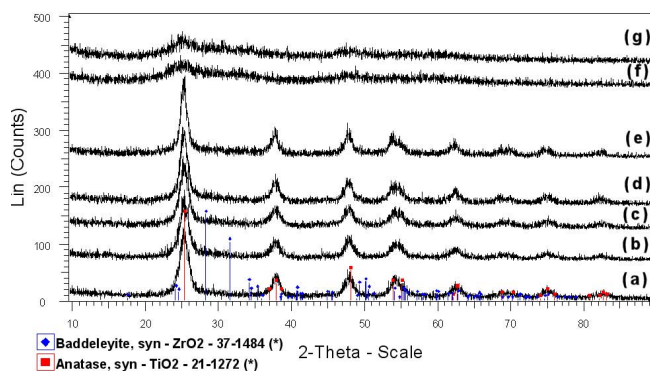
Fig. (1). XRD pattern of **a**) undoped TiO_2 denoted as TiZr_0, Zr^{4+} doped TiO_2 sample denoted as **b**) TiZr_1, **c**) TiZr_2, **d**) TiZr_3, **e**) TiZr_4, **f**) TiZr_5, **g**) TiZr_6.

3.2. Infrared spectroscopy (IR)

Figs. (**2a** and **2b**) show the IR spectrum of the Zr^{4+} doped titania and ZrO_2 as a reference sample (Fig. **2c**).

The broad absorption peaks about 3400 cm^{-1} and the band at 1630 cm^{-1} correspond to the surface absorbed water and the hydroxyl groups [30]. The small peak at ~ 1400 cm^{-1} can be assignet as absorbed carbonates on surfaces of TiO_2, formed by the adsorption of atmospheric CO_2 [31]. No other peaks are identified, therefore the Zr atoms substitue Ti atoms in the samples denoted TiZr_1-TiZr_4. The peak in the sample TiZr_5 (Fig. **2b**) corresponds with the broad peak in the sample of ZrO_2 (Fig. **2c**) and zirconium phase detected, which correspods with origin of amorphous phase (see XRD)
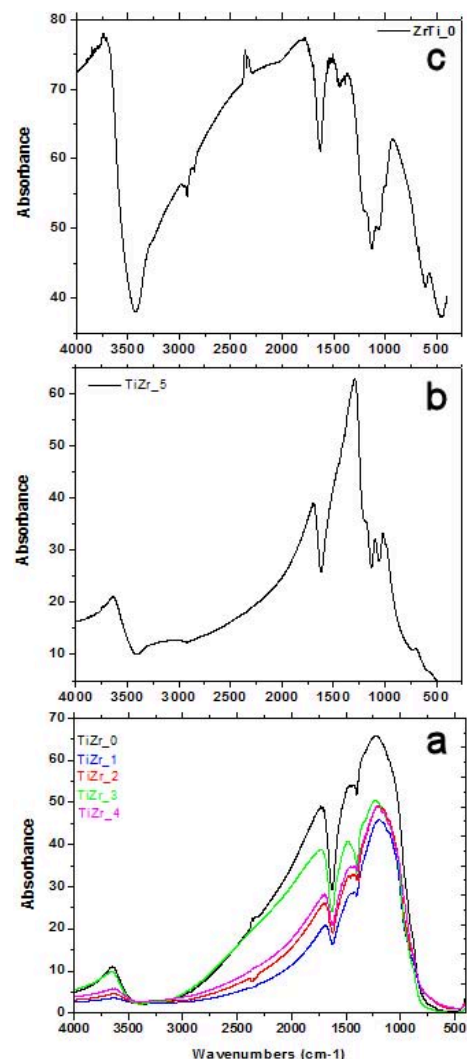
Fig. (2). Infrared spectrum of **a**) sample denoted TiZr_0-TiZr4, **b**) sample denoted TiZr_5, **c**) reference sample ZrO_2.

3.3. Scanning Electron Microscopy (SEM)

As it follows from the SEM micrographs, (see Fig. **3**), the synthesized samples of Zr-TiO_2 consist of spherical clusters of rather narrow size distribution: 1-2 µm in diameter. Based on the HRTEM results (see Fig. **4**), these spherical particles are formed by primary 4–5 nm anatase nanocrystals, interlayed by a small fraction of amorphous material. The EDX analysis of content Zr is presented in Table **1**.

3.4. Transmission Electron Microscopy (TEM and HRTEM)

Results obtained by high resolution transmission electron microscopy (HRTEM) and electron diffraction (ED) are shown in Figs (**4** and **5**), respectively. The HRTEM micrographs in Figs. (**4a-d**) characterized the surface morphology of the sample denoted TiZr_4. It is obvious that the sample TiZr_4 consists of very good crystallized nanosized titania. The interlayer spacing of d = 0.35 nm corresponds to the (101) plane of anatase (Fig. **4b**). Image processing analysis of HRTEM micrograph was used to achieve the refinement of microstructure in the sense that we can more accurately analyze single grains and grains boundaries. Furthermore,

from Fourier transform it is possible to determine and to index crystallographic planes and find their orientations. Fig. (**4c** and **4d**) show Fourier transform from the region of the original image taken with mask 512×512 pixels, these inserted areas correspond to (1 1 0) crystal plane of anatase.
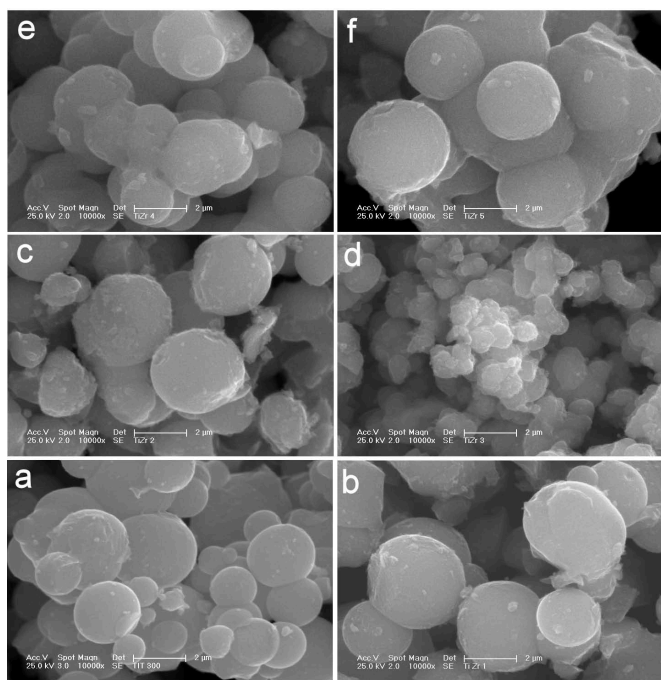
Fig. (3). SEM images of **a**) undoped TiO_2 denoted as TiZr_0, Zr^{4+} doped TiO_2 sample denoted as **b**) TiZr_1, **c**) TiZr_2, **d**) TiZr_3, **e**) TiZr_4, **f**) TiZr_5, **g**) TiZr_6.
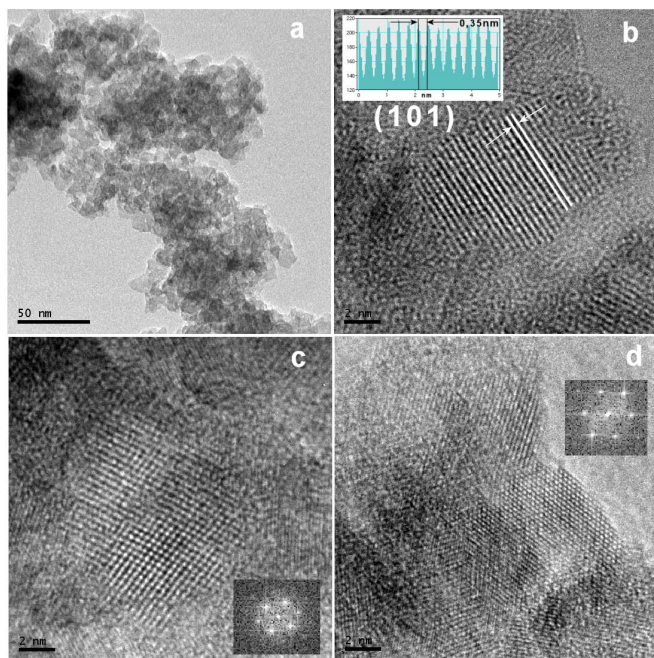
Fig. (4). HRTEM micrographs of Zr^{4+} doped titania denoted as TiZr_4, **a**) magnification 80 000, Images **b**, **c** and **d** are enlarged parts of the image (**a**).

Diffraction methods are the most important sources of structure information to identify individual microscopic-

sized crystallites, i.e. to identify the crystallographic phase the crystallite corresponds to. Structure determination is generally based on selected area electron diffraction (SAED) patterns in the transmission electron microscope (TEM). A computer program called ProcessDiffraction [32] helps indexing a set of single crystal selected area electron diffraction (SAED) patterns by determining which of the presumed structures can fit all the measured patterns simultaneously. Distances and angles are measured in the digitalized patterns with a graphical tool by clicking on the two shortest non-collinear vectors (spots), using user-supplied calibration data. Next figure (Fig. **5**) depicts the selected electron diffraction patterns (SAED) analyzed by ProcessDiffraction program and resulted that the structure of the sample is anatase (ICDD PDF 21-1272).
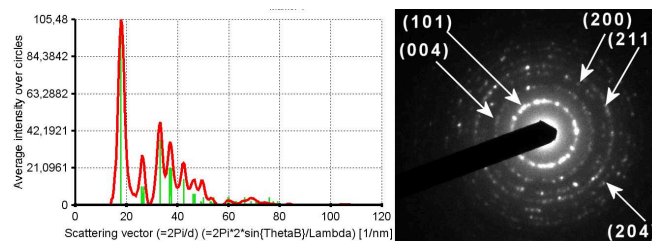
Fig. (5). Electron diffraction pattern of sample denoted as TiZr_4 (anatase). The ED pattern was treated using software Process Diffraction.

3.5. Surface Area and Porosity

BET surface area of Zr^{4+} doped titania depends on the amount of Zr, the largest surface area ($282.3 m^2 g^{-1}$) has a sample denoted as TiZr_4 (see Table **1**). All prepared samples displayed a type I isotherm with desorption hysteresis loop A [33]. A hysteresis type is due to cylindrical pores opened at both ends and the microporosity of pore size distribution is under pore diameter 6 nm. Results from desorption BJH pore volume distribution and pore area distribution confirmed microporous (> 2 nm) structure of prepared undoped titania and doped titania with content of Zr higher than 15 weight percent. The samples denoted as TiZr_1 - TiZr_4 embodied small growth of pores (~ 3 nm). The BJH method of desorption dV(r) versus pore radius and dS(r) versus pore radius for all prepared samples are presented in Fig. (**6**). Pore radius and pore volume are presented in Table **1**, pore volume increased with the content of Zr and maximum have the sample denoted as TiZr_1.

3.6. Degradation of Warfare Agents

The results of degradation of warfare agents, sulphur mustard, soman and matter VX, are presented in Fig. (**7**). The relevant detoxification capabilities of evaluated samples were expressed as percentages of the sulphur mustard (HD), soman (GD) and matter VX, respectively, degree of conversion. The undoped titania converted per 32 min sulphur mustard to 87.7 %, soman to 97.1 % and matter VX to 98.9%. Good results were obtained by the decomposition of sulphur mustard (see Fig. **7a**), where conversion comes to ~ 80 %. The best degradation properties (95.2%) has the sample denoted as TiZr_4. Excellent results were obtained for degradation of soman (Fig. **7b**.) and matter VX (Fig. **7c**). Total deg-

radation of soman or matter VX on Zr-doped titania run up through 1 minute. The best detoxification activity showed once again the sample denoted as TiZr_4. With the next increasing of content Zr decreases the decomposition of warfare agents due to the collapse crystallinity and break down of porosity. The presence of Zr^{4+}dopant therefore could suppress the growth of TiO_2 grains, increase the surface area, decrease the anatase–rutile phase transformation [34] and accelerate the surface hydroxylation. These properties, mainly surface hydroxylation, and high degradation activity of warfare agents for Zr^{4+} doped nano TiO_2 were resulted.
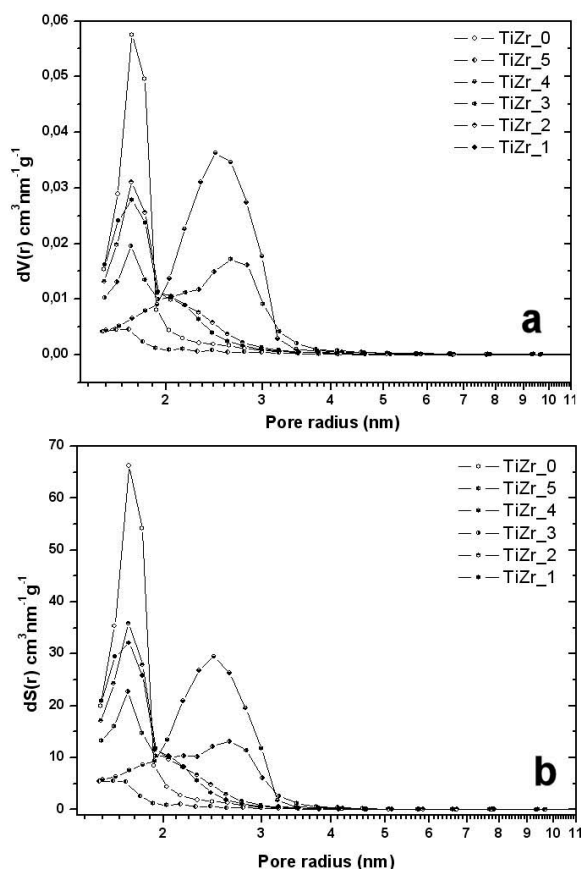
Fig. (6). BHJ pore size distribution **a**) dV(r) versus pore radius **b**) dS(r) versus pore radius.

3.7. Photocatalytic Activity

The photocatalytic activity of the prepared samples was determined by the degradation of 0.02 M Orange 2 dye aqueous solutions under UV radiation (at 254 nm and 365 nm). In the regions where the Lambert-Beer law is valid, the concentration of the Orange 2 dye is proportional to absorbance. The time dependences of Orange 2 dye decomposition can be described by using Equation (3) for the first kinetics reaction [35]:

$$\frac{d[OII]}{dt} = k\left(a_0 - [OII]\right) \qquad (2)$$

where [OII] is concentration of Orange 2 dye, a_0 is initial concentration of Orange 2 dye and k is rate constant. It is visible from Fig. (**8**), that the first order kinetics curves (plotted as lines) fitted to all experimental points. For comparison, the photocatalytic activity of a commercially available

photocatalyst (Degussa P25) and undoped anatase TiO_2 were also tested. The calculated degradation rate constants are listed in Table **1** and kinetic degradation of Orange 2 dye at 254 nm and 365 nm wavelength of the all prepared samples are presented in Fig. (**8**).
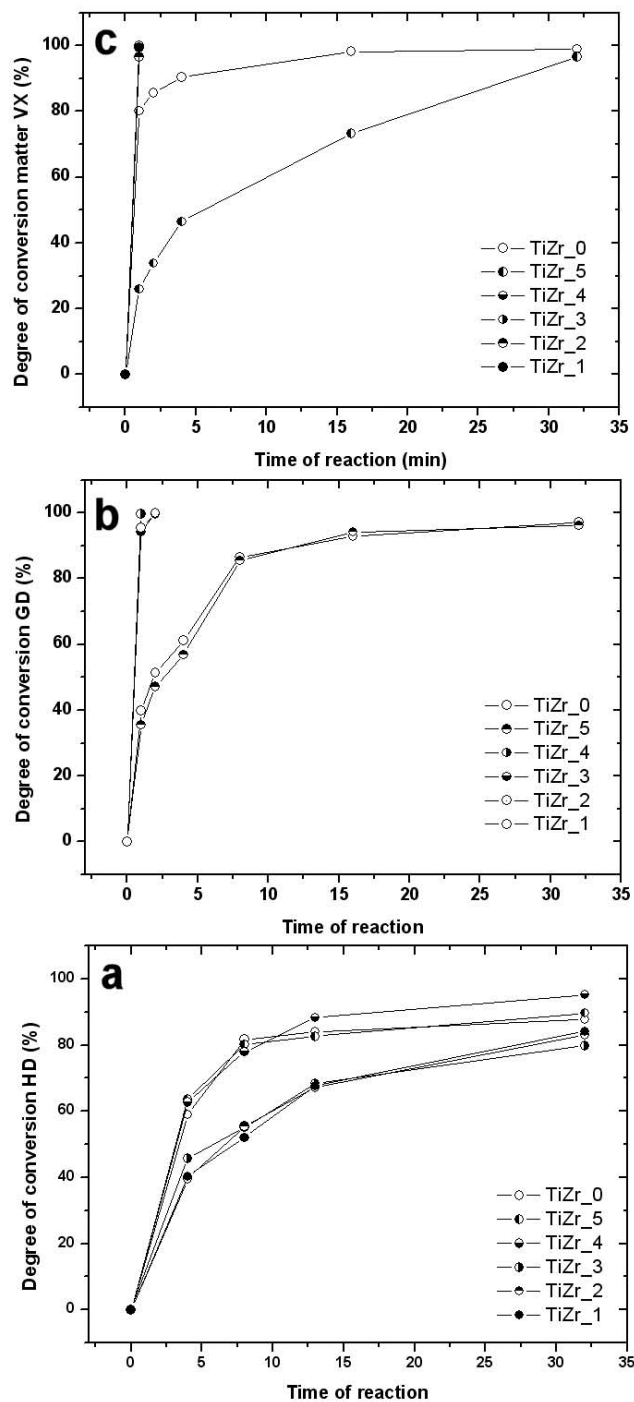
Fig. (7). Degree of conversion **a**) sulphur mustard (HD), **b**) soman (GD) **c**) matter VX on Zr^{4+} doped TiO_2.

From Table **1** follows, that pure undoped titania (sample denoted TiZr_0) exhibits higher photocatalytic activity for aqueous Orange 2 dye degradation than Zr doped samples. For pure TiO_2, the e^- and h^+ recombination may be grouped into two categories: volume recombination and surface recombination. Volume recombination is a dominant process

in well-crystallized large TiO_2 particles [36], which can be reduced by decreasing particle size. Reduction in particle size also leads to larger surface area, which increases the available surface active sites. Surface recombination becomes an important process when particle size becomes extremely small, about 1 nm [36]. In the as prepared samples, growth of concentration Zr to aprox. 13 weight % increased the sizes of the nanocrystals, higher concentration of Zr formed amorphous phases with particle size about 1 nm. Therefore, an optimal particle size exists in the pure TiO_2
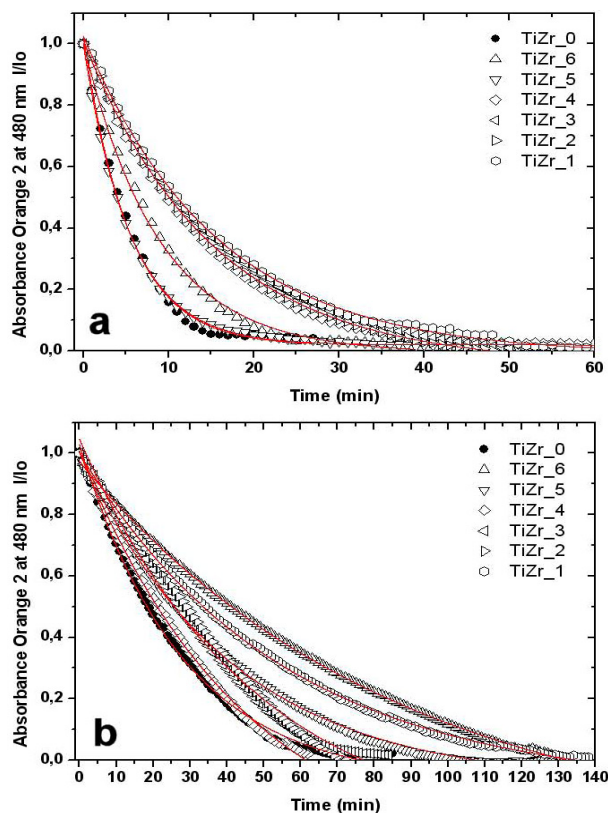
system for the maximum photocatalytic efficiency. The energy of a photon is related to its wavelength and the overall energy input to a photocatalytic process depends upon the light intensity. Therefore, the effect of both intensity and wavelength are important. Matthewes and mcEvoy [37] showed that shorter wavength (254 nm) radiation is considerably more effective in promoting degradation than radiation centred at 350 nm and the optimum rate occurred with a lower catalyst loading than required at 350 nm. As a rulel in laboratory condition the photocatalytic properties are measured at 365 nm, but for industrial purposes using of 254 nm wavelength is more effective.

CONCLUSION

In this paper, we have shown that particle size plays an important role in the properties of nanocrystalline TiO_2 as nanodispersive oxide for degradation of warfare agents and based photocatalysis, mostly through influencing the dynamics of e^- and h^+ recombination. We found out that doping Zr-TiO_2 prepared by homogeneous hydrolysis of titanium and zirconium oxo-sulphates mixture in aqueous solutions have positive influence to degradation activity of warfare agents and decreases photocatalytic degradation of Orange 2 dye. The presence of Zr^{4+} dopant, increases the surface area, crystallites size and accelerates the surface hydroxylation. Total degradation of soman or matter VX on Zr-doped titania run up through 1 minute is for sample with ~ 13.2 weight % Zr. The limitation of this work is using of obtained materials for warfare agents degradation only. The future direction of study should be focused on applying forenamed materials to purification of problematical and polluted environment [38, 39]. For example, using of ultra-filtration membrane fouling and pressure filter dewatering efficiency [40].

Fig. (8). Photocatalytic activity of Zr^{4+} doped TiO_2 **a**) at wavelengths 254 nm, **b**) at wavelengths 365 nm

Table 1. **Experimental Conditions, Crystallite Size, Cell Parameter *a* and *c* of TiO₂. Surface Areas and Porosity**

Sample	ZrOSO₄ [g]	EDX of Zr [wt .%]	Anatase Crystallite Size [nm]	Cell Par. *a*	Cell Par. *c*	BET [m²g⁻¹]	Pore Radius [Å]	Pore Volume [ccg⁻¹]	K at 254 nm [min⁻¹]	K at 368 nm [min⁻¹]
TiZr_0	0	-	4.2	3.7860	9.5148	200.4	17.344	0.190	0.1737	0.0434
TiZr_1	1	1.48	5.2	3.7987	9.5306	163.3	17.338	0.162	0.0669	0.0231
TiZr_2	3	6.78	5.4	3.8043	9.5597	167.2	17.292	0.169	0.0748	0.0318
TiZr_3	5	8.80	6.3	3.8129	9.5786	209.6	17.268	0.253	0.0693	0.0343
TiZr_4	10	13.17	7.2	3.8146	9.5860	282.3	24.640	0.352	0.0766	0.0400
TiZr_5	15	15.22	~ 1	-	-	26.5	17.122	0.028	0.1679	0.9799
TiZr_6	20	18.93	~ 1	-	-	211.6	16.349	0.201	0.1158	0.0195
P25	-	-	-	-	-	-	-	-	0.0539	0.0225

REFERENCES

[1]   Koper, O.; Lucas, E.; Klabunde, K.J. Development of reactive topical skin protectants against sulfur mustard and nerve agents. *J. App. Toxicol.*, **1999**, *19*, 59.

[2]   Koper, O.; Lucas, E.; Klabunde, K.J. *Oxide Nano particles as Countermeasures against Chemical and Biological Threats*, Proceedings of the joint service, chemical and biological decontamination conference, Salt Lake City (USA), **2000**.

[3]   Wagner, G.W.; Bartram, O.W. Reactions of the nerve agent simulant diisopropyl uorophosphate with self-decontaminating adsorbents. A P-31 MAS NMR study. *J. Mol. Catal. A Chem.*, **1999**, *144*, 419-424.

[4]   Wagner, G.W.; Bartram, O.W.; Koper, O.; Klabunde, K.J. Reactions of VX, GD and HD with nanosize MgO. *J. Phys. Chem. B*, **1999**, *103*, 3225 - 3228.

[5]   Wagner, G.W.; Koper, O.; Lucas, E.; Decker, S.; Klabunde, K.J. Reactions of VX, GD, and HD with nanosize CaO: Autocatalytic dehydrohalogenation of HD. *J. Phys. Chem. B*, **2000**, *104*, 5118-5123.

[6]   Štengl, V.; Bakardjieva, S.; Maříková, M.; Šubrt, J.; Opluštil, F.; Olšanská, M. Aerogel nanoscale magnesium oxides as a destructive sorbent for toxic chemical agents. *Cent. Eur. J. Chem.*, **2004**, *2*, 16-33.

[7]   Štengl, V.; Bakardjieva, S.; Maříková, M.; Šubrt, J.; Opluštil, F.; Olšanská, M. Aerogel nanoscale aluminium oxides as a destructive sorbent for mustard gas. *Ceramics-Silikaty*, **2003**, *47*, 175-180.

[8]   Šubrt, J.; Boháček, J.; Štengl, V.; Grygar, T.; Bezdička, P. Uniform particles with a large surface area formed by hydrolysis of Fe-2(SO4)(3) with urea. *Mater. Res. Bull.*, **1999**, *34*, 905-914.

[9]   Štengl, V.; Šubrt, J.; Bezdička, P.; Maříková, M.; Bakardjieva, S. Homogeneous precipitation with urea - An easy process for making spherical hydrous metal oxides. *Solid State Chem. V Solid State Phenomena*, **2003**, *90-91*, 121-126.

[10] Štengl, V.; Maříková, M.; Bakardjieva, S.; Šubrt, J.; Opluštil, F.; Olšanská, M. Reaction of sulfur mustard gas, soman and agent VX with nanosized anatase TiO_2 and ferrihydrite. *J. Chem. Tech. Biotech.*, **2005**, *80*, 754-758.

[11] Bakardjieva, S.; Šubrt, J.; Štengl, V.; Dianez, M.J.; Sayagues, M.J. Photoactivity of anatase-rutile TiO_2 nanocrystalline mixtures obtained by heat treatment of homogeneously precipitated anatase. *App. Catal. B-Environ.*, **2005**, *58*, 193-202.

[12] Daněk, O.; Štengl, V.; Bakardjieva, S.; Murafa, N.; Kalendová, A.; Opluštil, F. Nanodispersive mixed oxides for destruction of warfare agents prepared by homogeneous hydrolysis with urea. *J. Phy. Chem. Solids*, **2007**, *68*, 707-711.

[13] Venkatachalam, N.; Palanichamy, M.; Arabindoo, B.; Murugesan, V. Enhanced photocatalytic degradation of 4-chlorophenol by Zr^{4+} doped nano TiO_2. *J. Mol. Catal. A Chem.*, **2007**, *266*, 158-165.

[14] Wang, Y.M.; Liu, S.W.; Lub, M.K.; Wang, S.F.; Gub, F.; Gai, X.Z.; Cui, X.P.; Pan, J. Preparation and photocatalytic properties of Zr^{4+}-doped TiO_2 nanocrystals. *J. Mol. Catal. A Chem.*, **2004**, *215*, 137-142.

[15] Das, D.; Mishra, H.K.; Parida, K.M.; Dalai, A.K. Preparation, physico-chemical characterization and catalytic activity of sulphated ZrO_2-TiO_2 mixed oxides. *J. Mol. Catal. A Chem.*, **2002**, *189*, 271-282.

[16] Hirano, M.; Nakahara, C.; Ota, K.; Tanaike, O.; Inagaki, M. Photoactivity and phase stability of ZrO_2-doped anatase-type TiO_2 directly formed as nanometer-sized particles by hydrolysis under hydrothermal conditions. *J. Solid State Chem.*, **2003**, *170*, 39-47.

[17] Chang, S.; Doong, R. Characterization of Zr-Doped TiO_2 Nanocrystals prepared by a nonhydrolytic Sol-Gel method at high temperatures. *J. Phys. Chem. B*, **2006**, *110*, 20808-20814.

[18] Chen, H.R.; Shi, J.L.; Yu, J.; Wang, L.Z.; Yan, D.S. Synthesis of titanium-doped ordered porous zirconium oxide with high-surface-area. *Microporous Mesoporous Mater.*, **2000**, *39*, 171-176.

[19] Manríqueza, M.E.; López, T.; Gómeza, R.; Navarrete, J. Preparation of TiO_2-ZrO_2 mixed oxides with controlled acid-basic properties. *J. Mol. Catal. A Chem.*, **2004**, *220*, 229-237.

[20] Djur, W.; Pickering, S.; McGarry, D.; Glaude, P.; Tambuyser R.; Schuster K. The properties of zirconia powders produced by homogeneous precipitation. *Ceramics International*, **1995**, *21*, 195-206.

[21] Brunauer, S.; Emmett, P.H.; Teller, E. Adsorption of gases in multimolecular layers. *J. Am. Chem. Soc.*, **1938**, *60*, 309.

[22] Barret, E.P.; Joyner, L.G.; Halenda, P.P. The determination of pore volume and area distributions in porous substances. I. Computations from nitrogen isotherms. *J. Am. Chem. Soc.*, **1951**, *73*, 373.

[23] JCPDS PDF-2 release 2001, ICDD Newtown square, PA, USA.

[24] Scherrer, P. Estimation of size and internal structure of colloidal particles by means of Röntgen rays. *Gottinger Nachrichte*, **1918**, *2*, 98-100.

[25] Houšková, V.; Štengl, V.; Bakardjieva, S.; Murafa, N.; Balek, V.; Havlín, V. Optically transparent titanium dioxide particles incorporated in hydroxyethyl methacrylate thin layers. *J. Chem. Phys.*, in press.

[26] Monteagudo, J.M.; Durán, A. Fresnel lens to concentrate solar energy for the photocatalytic decoloration and mineralization of Orange 2 in aqueous solution. *Chemosphere*, **2006**, *65*, 1242-1248.

[27] Franke, S. Lehrbuch der Militarchemie, Militarverlag der Deutschen Demokkratischen Republik, **1976**.

[28] Ellman, G.L. A colorimetric method for determining low concentrations of mercaptans. *Arch. Biochem. Biophy.*, **1958**, *74*, 443-450.

[29] Shi, J.L.; Gao, J.H. Preparation of spherical zirconium salt particles by homogeneous precipitation, *J. Mat. Sci.*, **1995**, *30*, 793-799.

[30] Shao, G.; Zhang, X.; Zhong, Y. Peparation and photocatalytic activity of hierarchically mesoporous-macroporous TiO_2-xNx. *App. Catal. B Environ.*, **2008**, *82*, 208-218.

[31] Connor, P.A.; Dobson, K.D.; McQuillan, A.J. Infrared spectroscopy of the TiO_2/Aqueous solution interface. *Langmuir*, **1999**, *15*, 2402-2408.

[32] Labár, J.L. Consistent indexing of a (set of) single crystal SAED pattern(s) with the process diffraction program. *Ultramicroscopy*, **2005**, *103*, 237.

[33] Lowell, S.; Shields, J.E. Powder surface area and porosity, *Chapman Hall*, **1998**.

[34] Venkatachalam, N.; Palanichamy, M.; Arabindoo, B.; Murugesan, V. Enhanced photocatalytic degradation of 4-chlorophenol by Zr4+ doped nano TiO_2. *J. Mol. Catal. A Chem.*, **2007**, *266*, 158-165.

[35] Macounová, M.; Krýsová, H.; Ludvík, J.; Jirkovský, J. Kinetics of photocatalytic degradation of diuron in aqueous colloidal solutions of Q-TiO_2 particles. *J. Photochem. Photobiol. A Chem.*, **2003**, *156*, 273.

[36] Serpone, N.D.; Lawless, D.; Khairutdinov, R. Subnanosecond relaxation dynamics in TiO_2 colloidal sols (Particle Sizes R, =1.0-13.4 nm). Relevance to heterogeneous photocatalysis. *J. Phys. Chem.*, **1995**, *99*, 16655-16661.

[37] Matthews, R.W.; McEvoy, S.R. A comparison of 254 nm and 350 nm excitation of TiO_2 in simple photocatalytic reactors. *J. Photochem. Photobiol. A Chem.*, **1992**, *66*, 355-366.

[38] Chau, K.W. Transverse mixing coefficient measurements in an open rectangular channel. *Advanc. Environ. Res.*, **2000**, *4*, 287-294.

[39] Chau, K.W. Field measurements of SOD and sediment nutrient fluxes in a land-locked embayment in Hong Kong. *Advanc. Environ. Res.*, **2002**, *6*, 135-142.

[40] Chau, K.W. Investigation on effects of aggregate structure in water and wastewater treatment. *Water Sci. Tech.*, **2004**, *50*, 119-124.